Anterior corneal asphericity calculated by the tangential radius of curvature

Jinglu Ying
Bo Wang
Mingguang Shi

Anterior corneal asphericity calculated by the tangential radius of curvature

Jinglu Ying,[a] Bo Wang,[b] and Mingguang Shi[a]
[a]Department of Ophthalmology, The Second Affiliated Hospital of Wenzhou Medical College, XueYuan west Road 109, Wenzhou 325027, China
[b]Nanjing University of Finance and Economics, School of Applied Mathematics, Nanjing 210046, China

Abstract. We propose a method of calculating the corneal asphericity (Q) and analyze the characteristics of the anterior corneal shape using the tangential radius. Fifty-eight right eyes of 58 subjects were evaluated using the Orbscan II corneal topographer. The Q-values of the flat principal semi-meridians calculated by the sagittal radius were compared to those by the tangential radius. Variation in the Q-value with semi-meridian in the nasal and temporal cornea calculated by the tangential radius was analyzed. There were significant differences in Q-values ($P < 0.001$) between the two methods. The mean Q-values of the flat principal semi-meridians calculated by tangential radius with -0.33 ± 0.10 in the nasal and -0.22 ± 0.12 in the temporal showed more negative than the corresponding Q-values calculated by the sagittal radius. The Q-values calculated by tangential radius became less negative gradually from horizontal semi-meridians to oblique semi-meridians in both nasal and temporal cornea. Variation in Q-value with semi-meridian was more obvious in the nasal cornea. The method of calculating corneal Q using the tangential radius could provide more reasonable and complete Q-value than that by the sagittal radius. The model of a whole anterior corneal surface could be reconstructed on the basis of the above method. © *2012 Society of Photo-Optical Instrumentation Engineers (SPIE)*. [DOI: 10.1117/1.JBO.17.7.075005]

Keywords: anterior corneal asphericity; corneal model; corneal shape; sagittal radius; tangential radius.

Paper 11743 received Dec. 13, 2011; revised manuscript received May 2, 2012; accepted for publication May 30, 2012; published online Jul. 9, 2012.

1 Introduction

It is well established that the anterior surface of the cornea is the major refractive element of the human eye, being responsible for approximately 75% of the eye's total un-accommodated refractive power.[1] It is currently believed that the human anterior corneal shape is closely modeled by a conic section which can be fully described by the vertex radius of curvature (r_0) and a shape factor.[2,3] The shape factor of a conic represents the variation in curvature form the apex towards the periphery. Five different parameters are used to express the shape factor of a conic: the shape factor E and its derivatives p, the eccentricity e, the conic constant k, and asphericity Q. The formulas of conversion between them are: $E = e^2, Q = -e^2$, and $K = p = 1 + Q$. Figure 1(a) shows a conic section referred to Cartesian coordinates with the vertex at the origin O. The equation of the conic section is given by $Y^2 = 2r_0Z - pZ^2$, where the Z-axis is the optical axis, Y-value is the semi-chord diameter, and Z-value is the sagittal depth of the section.[4,5] A conic section is obtained by cutting a cone by a plane including sphere, ellipse, hyperbola, and parabola [Fig. 1(b)]. Figure 1(b) is a version of Figure 5.14 from Smith and Atchison's book, "*The Eye and Visual Optical Instruments.*"[6] Bennett[7] derived the conic equation $r_s^2 = r_0^2 + (1 - p)y^2$ to calculate the p-value by sagittal radius (r_s) from keratometry. Since then, many researchers have studied the corneal shape by asphericity (p or Q) calculated by sagittal radius according to Bennett's equation.[8–12]

Figure 2 represents a conicoidal corneal section in any given meridian in contact with a sphere at P and P'. At any off-axis point such as P there are two principal curvatures, the sagittal and the tangential. They can be obtained respectively from the axial power map and tangential power map in current corneal topography. The sagittal section is perpendicular to the tangential section containing the optical axis ZZ. The sagittal radius of curvature (r_s) in sagittal section refers to the distance PC_s along the normal from the corneal surface to the optic axis ZZ. The tangential radius of curvature (r_t) in the tangential section, also known as the instantaneous radius of curvature refers to the distance, PC_t. The tangential curvature is referred to as axis independent, because the center of curvature does not have to lie on the optical axis.[13–15]

The asphericity (Q) calculation by sagittal radius (r_s) has been reported from previous studies. However, the sagittal radius (r_s) is spherically biased, and is not a true radius of curvature.[13–15] Tangential radius (r_t) is a true radius which can better represent corneal shape and local curvature changes especially in the periphery.[16] To our knowledge, there is no report of investigating the corneal asphericity (Q) calculation by r_t. In the present study, we evaluate corneal shape by Q calculated by r_t for the first time. The purposes of this study was to assess the difference of Q-values in the flat principal semi-meridians between that calculated by the sagittal radius (r_s) and tangential radius (r_t), respectively. We also analyzed the characteristics of the Q-values calculated by the tangential radius (r_t) in the nasal and temporal cornea. By calculating 360 Q-values of semi-meridians, we explored the reconstruction of an accurate model of a whole anterior corneal surface.

Address all correspondence to: Mingguang Shi, The Second Affiliated Hospital of Wenzhou Medical College, Department of Ophthalmology, XueYuan west Road 109, Wenzhou, 325027, China. Tel.: +86-577-88879100; Fax: +86-577-88879100; E-mail: pshimg2010@hotmail.com
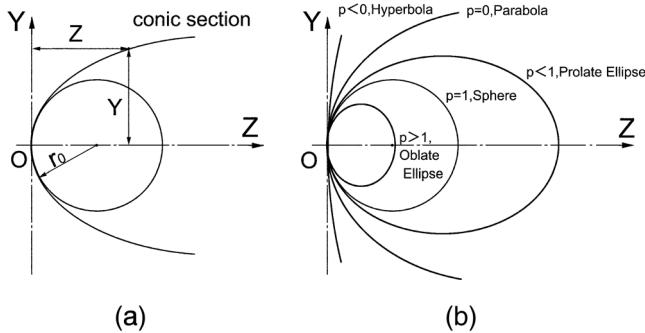
(a)   (b)

Fig. 1 The general equation to all of the conic section is given by $Y^2 = 2r_0Z - pZ^2$ (a) and the family of conic sections of asphericity p (b) (Fig. 5.14, Ref. 5).
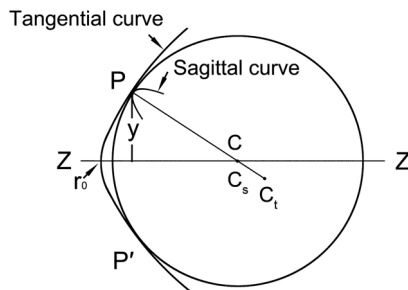

Fig. 2 Schematic of a section in any given meridian through a conicoidal corneal surface in contact with a sphere at the points P and P'.

2 Subjects and Methods

2.1 Aspheric Test Objects

Ten conicoidal surface convex aspheric test objects were manufactured to produce surfaces similar to normal human cornea. The material of these aspheric test objects was polymethylmethacrylate (PMMA). The test objects had well-defined convex aspheric surfaces (vertex radius $r_{0\text{preset}}$ and asphericity Q_{preset}), a diameter of 10 mm, and were manufactured using an ultra-precision diamond turning lathe (AMETEK. Sterling.

Precitech, Inc). The test objects were all verified by the Form TalySurf PGI840 (Taylor Hobson Ltd., Leicester, UK) and measured in 1 meridian marked by the engraved line, which was horizontal. Then, the test objects were mounted on a matt black holder and subjected to three measurements using the Orbscan II topographer (version 3.00). The Q-value and r_0-value of horizontal meridian of each test object were calculated by sagittal radius and tangential radius. Data collection of Orbscan II and calculation of Q-value and r_0-value by the two methods is introduced in following section in detail.

2.2 Subjects

Fifty-eight right eyes of 58 normal emmetropic subjects (29 females and 29 males) were evaluated. The mean age of the subjects was 24 years ±4.04 (SD) (range: 18 to 36 years). Inclusion criteria were the spherical equivalent refractive error more than -0.25DS and less than $+0.50$DS, corneal astigmatism less than 1.00DC, and absence of ocular disease and previous refractive surgery. The study followed the tenets of the Declaration of Helsinki. Informed consent was obtained from all subjects.

2.3 Data Collection

The Orbscan II corneal topographer was used to acquire three independent images of the topography of the right eye of each subject and test objects. All three images were acquired by the same examiner. The raw data of the topography map were downloaded onto a compact disk in .txt file format, which contained the dioptric power (P) of data points of the anterior corneal surface from both axial and tangential power maps. Figure 3 shows an example of axial power map (a) and tangential power map (b) of the right eye for subject no. 4. The perpendicular distance from the point to optical axis was defined as y (Fig. 2). A series of points on a semi-meridian section were arranged at 0.1-mm intervals. The interval between two semi-meridians was 1 deg. The sagittal radius (r_s) and tangential radius (r_t) were obtained using the corneal refractive index of 1.376, and the equation $r = 376/P$.[17] The flat principal meridian was selected by keratometry for examination.
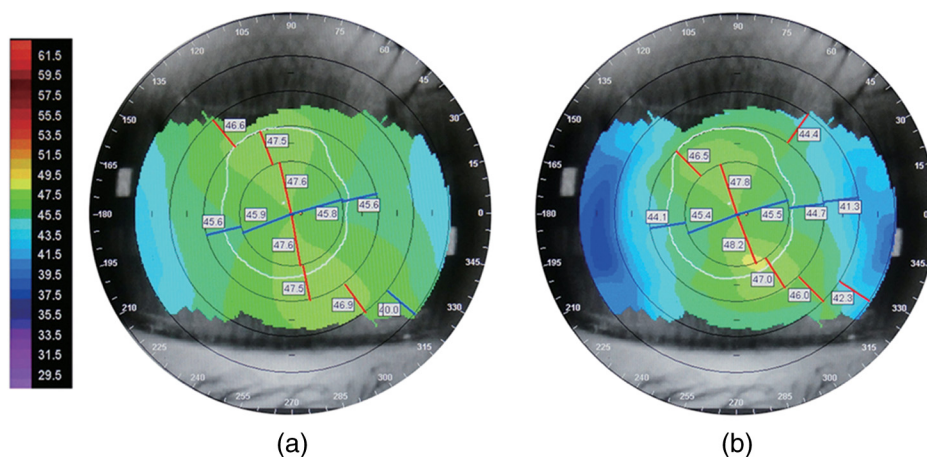

(a)   (b)

Fig. 3 An example of axial power map (a) and tangential power map (b) of the right eye for subject no. 4.

2.4 Q-Value Calculation by Sagittal Radius According to Bennett's Equation

Bennett[6] derived the equation for conic section as following:

$$r_s^2 = r_0^2 + (-Q)y^2, \qquad (1)$$

where r_s, r_0, Q, and y refer to the sagittal radius, the vertex radius, corneal asphericity (Q), and perpendicular distance from the point to optical axis, respectively. Douthwaite[18] used the linear regression method to plot a straight line graph of r_s^2 (on the ordinate) versus y^2 (on the abscissa). The square root of the intercept on the ordinate equals r_0, and the negative slope of the line equals Q. The straight line gives a coefficient of determination (R^2). The Q-value and r_0-value of the flat principal meridian of human eyes and horizontal meridian of test objects were calculated by the points on the axial power map, from the first point at 0.1 mm to the most peripheral point. The means of three Q-values and three r_0-values were regarded as the resulting value.

2.5 Q-Value Calculation by Tangential Radius According to the Implicit Function Differential Method

A three dimensional Cartesian coordinate system is set with its origin at vertex normal to the corneal intersection of the optic axis of the videokeratoscopy.[19] The Z-axis, Y-axis, X-axis of the coordinate represent the optical axis direction, the vertical direction and the horizontal direction, respectively. θ is the angle between the corneal meridian section and the XOZ plane. The corneal meridian section is located on the YOZ plane when $\theta = 90$ deg, and it can be correspondingly described by the conic equation: $y^2 = a_1 z + a_2 z^2$, while situated on the XOZ plane when $\theta = 0°$ and described by the conic equation: $x^2 = a_1 z + a_2 z^2$. For any other angle θ except for 0, 90, 180, and 270 deg., the YOZ plane can be coincided with the θOZ plane by rotating the coordinate system. Thus the corneal meridian section of any other angle θ can also be described by the conic equation $y^2 = a_1 z + a_2 z^2$ in the new coordinate system.

Let us take corneal meridian section with $\theta = 90$ deg, for example. The formula of the curvature of a point on the section can be expressed as:

$$K = \frac{1}{r_t} = \frac{|y''|}{\sqrt{[1 + (y')^2]^3}}, \qquad (2)$$

where y' and y'' are the first and second derivatives with respect to z, which is a Z-axis coordinate value of the point. Differentiating both sides of the conic equation $y^2 = a_1 z + a_2 z^2$ with respect to z, we get

$$y' = \frac{a_1 + 2a_2 z}{2y}, \quad y'' = \frac{-a_1^2}{4y^3}.$$

Then by substituting y' and y'' into Eq. (2), we obtain:

$$r_t = \frac{4}{a_1^2} \left[\frac{a_1^2}{4} + (1 + a_2)y^2 \right]^{\frac{3}{2}}. \qquad (3)$$

Since $Q = -e^2$ in which e is eccentricity and equals the focal length divided by the major axis length of the conic curve, $Q = -(1 + a_2)$. r_0 can be calculated by setting $y = 0$ from Eq. (3), so that $r_0 = a_1/2$. Finally by substituting $a_1 = 2r_0$ and $a_2 = -(1 + Q)$ into Eq. (3), we obtain the following equation:

$$r_t = \frac{1}{r_0^2} [r_0^2 - Qy^2]^{\frac{3}{2}}, \qquad (4)$$

where r_t, r_0, Q, and y refer to the tangential radius, the vertex radius, corneal asphericity (Q), and perpendicular distance from the point to optical axis, respectively.

Since r_t is a nonlinear function of y in Eq. (4), it is difficult to calculate r_0 and Q. To transform the nonlinear problem to the linear problem, Eq. (4) is converted to another form which can be written as:

$$y^2 = b + c r_t^{\frac{2}{3}}, \qquad (5)$$

where b and c are constants, a straight line graph of y^2 (on the ordinate) versus $r_t^{2/3}$ (on the abscissa) is plotted. By the linear regression method, we get $b = r_0^2/Q$ and $c = -(r_0^{4/3}/Q)$, that is, $Q = r_0^2/b$ and $r_0 = [-(b/c)]^{3/2}$. The straight line also gives a coefficient of determination (R^2). The Q-value and r_0-value of the given meridian of human eyes and horizontal meridian of test objects were calculated by the points on the tangential power map, from the first point at 0.1 mm to the most peripheral point. The means of three Q-values and three r_0-values were regarded as the resulting value.

2.6 Comparison of Precision Between Two Q-Values by Sagittal Radius and Tangential Radius

Perturbation analysis was used to assess the precision of Q-values calculation between the two methods. The two sides of both equations [see Eqs. (1) and (4)] were differentiated separately. We obtained equations as following:

$$dQ_s = \frac{2r_s}{y^2} dr_s. \qquad (6)$$

$$dQ_t = -\frac{4r_0^2 dr_t}{6(r_t r_0^2)^{\frac{1}{3}} y^2}. \qquad (7)$$

Then Eq. (6) was divided by Eq. (7). Since r_s/r_0 and r_t/r_0 equals to 1 approximately. So assuming $dr_s = dr_t$, we obtained:

$$\left| \frac{dQ_s}{dQ_t} \right| = 3 \cdot \frac{r_s}{r_0} \cdot \left(\frac{r_t}{r_0} \right)^{\frac{1}{3}} \approx 3. \qquad (8)$$

The implication of Eq. (8) will be explained in detail later (see Discussion, Sec. 4 below).

2.7 Repeatability of Q and r_0 Calculations using Orbscan II

Douthwaite[20] suggested that a three measurement average should be a representative result for Q and r_0 for single meridian measurements using Orbscan II to improve repeatability. In our study, intrasession and intersession repeatability of Q and r_0 of the temporal flat principal semi-meridian using Orbscan II with the two methods were assessed in a subset of 20 right eyes of 20 subjects. In the first session, three repeated measurements were obtained for intrasession repeatability analysis. Measurements were repeated in a second session at the same time on the third day for intersession repeatability.

2.8 Analysis

The nasal cornea includes quadrant I (0–11, 11–20, 21–30, and 31–50 deg.) and quadrant IV (350–359, 340–349, 330–339, and 310–329 deg.). The temporal cornea includes quadrant II (170–180, 160–169, 150–159, and 130–149 deg.) and quadrant III (181–190, 191–200, 201–210, and 211–230 deg.).

Statistical analysis was performed using SPSS software (version 17.0, SPSS, Inc.). The Kolmogorov-Smirnov test was used to check normal distribution of data. The level of significance was set at five percent. The differences in r_0-value and Q-value of test objects between predefined values and those calculated by the two methods were compared using a repeated measures analysis of variance (ANOVA). The intrasession repeatability was tested using the intraclass correlation coefficient (ICC)[21] and coefficient of variation (CV). The intersession repeatability was defined as twice the standard deviation (SD) of the difference between the mean of three measurements in the two sessions according to The British Standard Institution.[22] Differences between Q-values and between r_0-values of the flat principal semi-meridians by the two methods were compared by paired t-tests. In linear regression analysis, the regression coefficient was tested by the ANOVA. Considering the reliability of linear regression equation, the coefficient of determination (R^2) should be more than 0.5.

3 Results

The Kolmogorov-Smirnov test showed that all parameter distributions were not significantly different from normal, with the exception of the coefficients of determination in the flat principal semi-meridians with the two methods. The linear regression equation had statistical significance. In all subjects, the flat principal meridians were within 10 deg.

3.1 Aspheric Test Objects

Table 1 shows results of the horizontal meridian of each test object calculated by sagittal radius and tangential radius using Orbscan II measurement. A repeated measures ANOVA, with a Bonferroni correction for multiple comparisons, for r_0-value ($P < 0.001$) indicates the differences between the predefined values and the values calculated by the two methods are significant. The ANOVA results for Q-value show no significant difference between the predefined values and those calculated by tangential radius ($P = 1.0$), while values calculated by sagittal radius showed a significant difference from the other two values ($P = 0.000$). Table 2 shows the mean of the differences in vertex radius Δr_0 and asphericity ΔQ of the test objects compared to the predefined values, $r_{0\text{preset}}$ and Q_{preset}. The mean differences between the values calculated by sagittal radius and the predefined values were approximately 1.48 times larger for $\Delta r_{0\text{sagittal}}$ and approximately 3.47 times larger for $\Delta Q_{\text{sagittal}}$ than the mean differences of the values calculated by tangential radius. Statistically significant differences were found between $\Delta r_{0\text{sagittal}}$ and $\Delta r_{0\,\text{tan gential}}$ ($P = 0.039$) and between $\Delta Q_{\text{sagittal}}$ and $\Delta Q_{\text{tan gential}}$ ($P < 0.001$).

3.2 Repeatability of Orbscan II Assessment of Q and r_0

The Orbscan II intrasession repeatability of Q and r_0 in the temporal flat principal semi-meridian calculated by the tangential radius were very reliable (Q's ICC: 0.91; CV = 2.23%.r_0's

Table 1 Results of measurement of the horizontal meridian of test objects calculated by sagittal radius and tangential radius.

		Calculated value from Orbscan II measurement			
Preset value		Sagittal		Tangential	
$r_{0\,\text{preset}}$	Q_{preset}	$r_{0\,\text{sagittal}}$	Q_{sagittal}	$r_{0\,\text{tan sagittal}}$	$Q_{\text{tan sagittal}}$
7.2	−0.20	7.26	−0.12	7.15	−0.18
7.6	−0.41	7.65	−0.28	7.56	−0.44
7.7	−0.30	7.73	−0.24	7.66	−0.32
7.7	−0.49	7.75	−0.37	7.69	−0.46
7.8	−0.25	7.85	−0.11	7.75	−0.20
7.8	−0.41	7.86	−0.31	7.77	−0.45
7.9	−0.30	7.94	−0.22	7.89	−0.33

Table 2 Differences in vertex radius (r_0) and asphericity (Q) of test objects.

| | Difference from preset value | | | |
| | Sagittal | | Tangential | |
Parameter	$\Delta r_{0\,sagittal}$	$\Delta Q_{sagittal}$	$\Delta r_{0\,tan\,sagittal}$	$\Delta Q_{tan\,sagittal}$
Mean	0.043	0.104	0.030	0.030
Standard deviation	0.013	0.025	0.015	0.012

Note: Δ = difference.

ICC: 0.948; CV = 1.50%). The results for Q and r_0 calculated by the sagittal radius were similar (Q's ICC: 0.893; CV = 2.59%. r_0's ICC: 0.95; CV = 1.73%). The Orbscan II intersession repeatability was 0.050 mm for Q and 0.076 mm for r_0 in the temporal flat principal semi-meridian calculated by the tangential radius, and 0.060 mm for Q and 0.074 mm for r_0 calculated by the sagittal radius. Both calculation methods demonstrated a high repeatability.

3.3 Function Relationship

The most peripheral points of the semi-meridians in the oblique semi-meridian regions were more than 3.5 mm departed from the corneal center and almost up to 4.5 mm in the horizontal semi-meridian regions. Figure 4 shows the dioptric power distributions against the distance (y) at 0.1 mm intervals in the nasal flat principal semi-meridian from both axial and tangential power maps respectively for the right eye of subject no. 1. Figure 5 illustrates a function scatterplot of the nasal flat principal semi-meridian of the right eye of the same subject with the implicit function differential method.

3.4 Coefficients of Determination

The median values of coefficients of determination (R^2) in the flat principal semi-meridians of the right eye with the two methods were above 0.9. The mean values of R^2 in the nasal and temporal of the right cornea with the implicit function differential method were above 0.83.
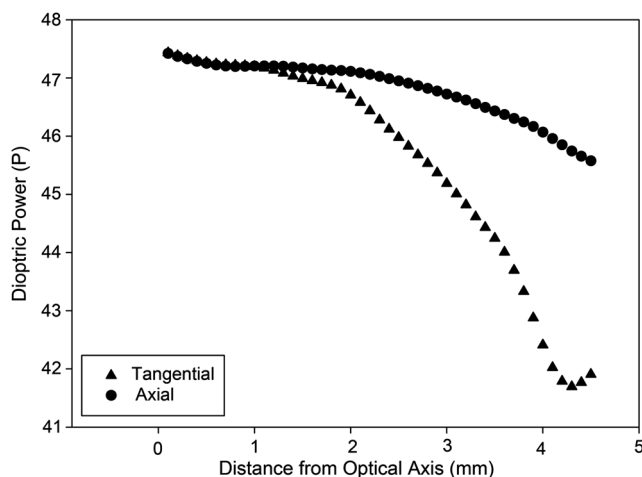

Fig. 4 Corneal tangential and axial dioptric power distributions as a function of distance from the optical axis in the nasal flat principal semi-meridian for the right eye of subject no. 1.
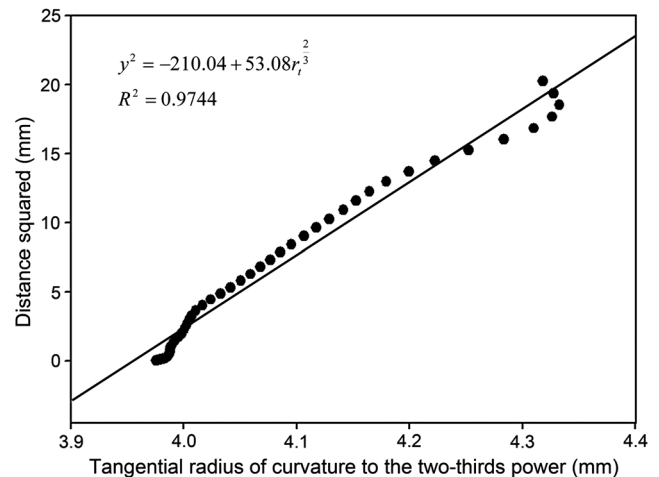

Fig. 5 Scatterplot of distance squared versus tangential radius to the two-thirds power in the nasal flat principal semi-meridian of the right eye for subject no. 1 with the implicit function differential method.

3.5 Comparison of Q-Values and r_0-Values in Flat Principal Semi-Meridians

Table 3 shows the mean Q-values and r_0-values in the flat principal semi-meridians calculated by sagittal and tangential radius. There were significant differences in Q-values ($P < 0.001$) and r_0-values ($P < 0.001$) between the two methods. The mean Q-values of the flat principal semi-meridians by the tangential radius were -0.33 ± 0.10 in the nasal and -0.22 ± 0.12 in the temporal, respectively. The Q-values were more negative when calculated by the tangential radius than the sagittal radius. The mean r_0-values of the flat principal semi-meridians calculated by the tangential radius were 7.83 ± 0.24 mm in the nasal and 7.80 ± 0.20 mm in the temporal, respectively, which were much smaller than those calculated by the sagittal radius.

3.6 Q-Values from Horizontal to Oblique Semi-Meridian Regions by Tangential Radius

Tables 4 and 5 show mean values for Q in the nasal and temporal of the cornea, respectively, at different semi-meridian regions. Table 3 shows the ranges of variation in Q-values from horizontal to oblique semi-meridian regions were -0.34 to -0.27 in quadrant I and -0.33 to -0.19 in quadrant IV. Table 4 shows the ranges of variation in Q-values from horizontal to oblique semi-meridian regions were -0.20 to -0.18 in quadrant II and -0.23 to -0.21 in quadrant III. The Q-values became gradually less-negative from horizontal to oblique

Table 3 Values for asphericity (Q) and vertex radius of curvature (r_0) in flat principal semi-meridians calculated by sagittal and tangential radius of curvature.

		Sagittal	Tangential	N	P
Q	Nf	-0.30 ± 0.11	-0.33 ± 0.10	57	<0.001
Q	Tf	-0.16 ± 0.09	-0.22 ± 0.12	51	<0.001
r_0	Nf	7.87 ± 0.23	7.83 ± 0.24	57	<0.001
r_0	Tf	7.86 ± 0.21	7.80 ± 0.20	51	<0.001

Note: Nf: Nasal flat principal semi-meridian; Tf: Temporal flat principal semi-meridian. n = number of eyes.

Table 4 Values for asphericity (Q) in the nasal cornea at different corneal semi-meridian regions.

Nasal	Corneal semi-meridian region (degrees)							
	310–329	330–339	340–349	350–359	0–10	11–20	21–30	31–50
	($n = 56$)	($n = 58$)	($n = 58$)	($n = 58$)	($n = 58$)	($n = 58$)	($n = 58$)	($n = 57$)
Mean $\pm$ SD	-0.19 ± 0.07	-0.25 ± 0.12	-0.30 ± 0.13	-0.33 ± 0.12	-0.34 ± 0.10	-0.33 ± 0.12	-0.31 ± 0.13	-0.27 ± 0.13
Range	-0.35 to -0.08	-0.53 to -0.08	-0.70 to -0.08	-0.64 to -0.10	-0.53 to -0.14	-0.64 to -0.13	-0.62 to -0.12	-0.66 to -0.14

Note: n = number of eyes; SD = standard deviation.

Table 5 Values for asphericity (Q) in the temporal cornea at different corneal semi-meridian regions.

Temporal	Corneal semi-meridian region (degrees)							
	130–149	150–159	160–169	170–180	181–190	191–200	201–210	211–230
	($n = 55$)	($n = 58$)	($n = 58$)	($n = 58$)	($n = 58$)	($n = 58$)	($n = 58$)	($n = 57$)
Mean $\pm$ SD	-0.18 ± 0.09	-0.20 ± 0.10	-0.20 ± 0.11	-0.20 ± 0.11	-0.22 ± 0.12	-0.23 ± 0.13	-0.23 ± 0.11	-0.21 ± 0.08
Range	-0.39 to -0.06	-0.46 to -0.08	-0.49 to -0.06	-0.55 to -0.07	-0.58 to -0.07	-0.65 to -0.06	-0.57 to -0.07	-0.45 to -0.09

Note: n = number of eyes; SD = standard deviation.

semi-meridian regions in the nasal and temporal cornea. The Q-values in the nasal cornea were more negative than those in the temporal cornea. Figure 6 shows the variation in asphericity with semi-meridian region in the nasal cornea of the right eye. Figure 7 shows the variation in asphericity with semi-meridian region in the temporal cornea of the right eye. It appeared there was no significant variation in Q-values with semi-meridian region in the temporal cornea. However, the nasal cornea showed obvious variation with semi-meridian region. The maximal difference between the Q-values of the semi-meridian regions in the nasal cornea was 0.15, while it decreased to 0.05 in the temporal cornea.

3.7 r_0-Values from Horizontal to Oblique Semi-Meridian Regions by Tangential Radius

The variations in r_0-values from horizontal to oblique semi-meridian regions were 7.83 to 7.80 mm in quadrant I, 7.82 to 7.78 mm in quadrant IV, 7.77 to 7.72 mm in quadrant II, and 7.79 to 7.76 mm in quadrant III. We found that the r_0-values

became smaller from horizontal to oblique semi-meridian regions in the nasal and temporal of the cornea. The r_0-values in the nasal cornea were much greater than those in the temporal cornea. The maximal difference between the r_0-values of the semi-meridian regions was 0.05 mm in the nasal cornea and 0.07 mm in the temporal cornea.

4 Discussion

4.1 Aspheric Test objects

The Q-value calculated by tangential radius was not significantly different to the predefined values, but the Q-value calculated by sagittal radius under-read compared to the predefined values. The r_0-value calculated by sagittal radius over-read, while that calculated by tangential radius under-read compared to the predefined values. The mean of the differences in r_0-value (Δr_0) and Q-value (ΔQ) between the values calculated by sagittal radius and the predefined values were both larger than the mean differences of the values calculated by tangential radius.
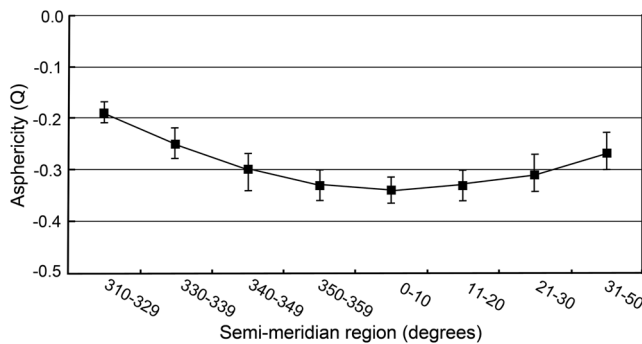
Fig. 6 Variation in asphericity as a function of semi-meridian region in the nasal cornea of the right eye. Bars denote 95% confidence interval (CI).
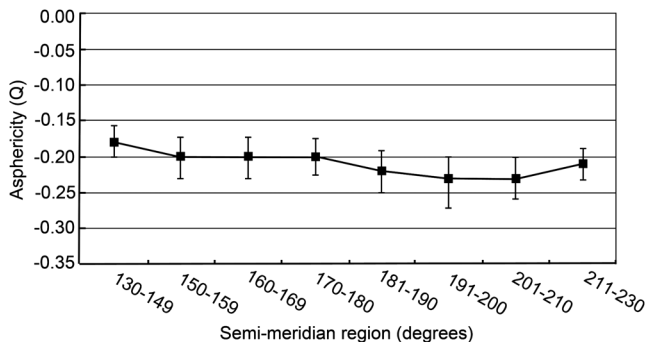

Fig. 7 Variation in asphericity as a function of semi-meridian region in the temporal cornea of the right eye. Bars denote 95% confidence interval (CI).

This result further indicates the tangential radius of curvature (r_t) is a true radius of curvature which can represent corneal shape more accurately.

4.2 Repeatability of Q-Value Calculations using Orbscan II

The Q- and r_0-value calculations with the sagittal radius have been used by many researchers previously. From the results of our study, we believe the Q- and r_0-value calculations with the tangential radius using Orbscan II are as reliable as those calculated with the sagittal radius. The repeatability of Q calculated by the tangential radius may be much better.

4.3 Optical Principle of Calculating Q-Value

Since Bennett[7] introduced the equation $rs^2 = r_0^2 + (1-p)y^2$ to calculate asphericity (p) by sagittal radius measured from keratometry, the equation has been accepted until now, particularly when used in any kind of videokeratoscope to calculate corneal asphericity. Many researchers studied the corneal asphericity which calculated by sagittal radius (r_s) according to Bennett's equation.[8–12] But there are two differences between the two methods. First, the sagittal radius used by Bennett to calculate the asphericity (p) is in the sagittal plane perpendicular to the tangential plane. Bennett supposed the center of the sagittal radius to intersect with the optical axis (Fig. 2). However, the human cornea is not a rotationally symmetric surface, so the center of the sagittal radius does not always lie on the optical axis. The sagittal radius can be obtained from the axial power map in corneal topography. However, the

axial curvature does not really measure the curvature of the cornea in any direction.[23] Thus, r_s is spherically biased and not a true radius of curvature,[13–15] and it will lead to erroneous result for an asymmetric corneal surface. The corneal surface consists of a series of tangential sections containing the optical axis. The method we introduced to calculate the Q-value used the tangential radii in the tangential section. The tangential radius of curvature (r_t) is a true radius of curvature which can better represent corneal shape and it can identify localized curvature changes sensitively in the peripheral cornea.[16] We believe the asphericity of the corneal surface calculated by tangential radius is more reasonable.

The second difference is Bennett's equation did not involve the rotation of the coordinate system. It could only be used to calculate Q-values of the principal semi-meridians or the principal semi-axes. Although the Q-value calculation of our method is more complex because the center of the tangential radius of a point on any given meridian section is outside the optical axis, this method can not only calculate Q-values of four principal semi-axes, but it can also calculate Q-values of other semi-meridians. In our study, Q-values of semi-meridians at 1-deg. intervals were calculated by tangential radius with 122 Q-values of horizontal semi-meridians and 80 Q-values of oblique semi-meridians. It follows that we could analyze the characteristics of the anterior corneal surface according to the relationship between Q-values of different semi-meridian regions.

4.4 Perturbation Analysis

Table 3 tells us that the Q-values calculated by the tangential radius were more negative than the Q-values calculated by sagittal radius in the flat principal semi-meridians. It was coincident with the trend of dioptric power distribution in Fig. 4 showing the flattening of the dioptric power from center to periphery on the tangential power map more obviously than that on the axial power map. Mathematically, we compared precision between two Q-values by sagittal radius and by tangential radius with perturbation analysis. Equation (8) indicates the change of Q caused by the change of r_s is three times greater than that caused by the change of r_t, assuming the change of r_s and r_t are equal. Here, the change of radius of curvature refers to the error between the measured value and true value. Therefore, the change of Q-value caused by the minor change of radius of curvature with the tangential radius is less than that with the sagittal radius. We suggest that the Q-value calculation by tangential radius can represent more accurate asphericity of corneal section.

4.5 Distribution of Q-Values by Tangential Radius

From Tables 4 and 5 and Figs. 6 and 7, the characteristics of the anterior corneal surface are as follows. First, the Q calculated by tangential radius in the nasal and temporal of the cornea for the sample analyzed in our study displayed negative values ($-1 < Q < 0$) corresponding to the most common corneal shape (prolate ellipse).[24] Second, the Q-values in the nasal cornea were more negative than in the temporal cornea. Thus, the nasal cornea has greater asphericity than the temporal cornea, and the ellipse shapes of semi-meridian regions between the nasal and temporal of the cornea are not symmetric. Third, the Q-values became less negative gradually from horizontal semi-meridian regions to oblique semi-meridian regions. This variation trend is more obvious in the nasal cornea than in the temporal cornea. However, the variation in Q-value with
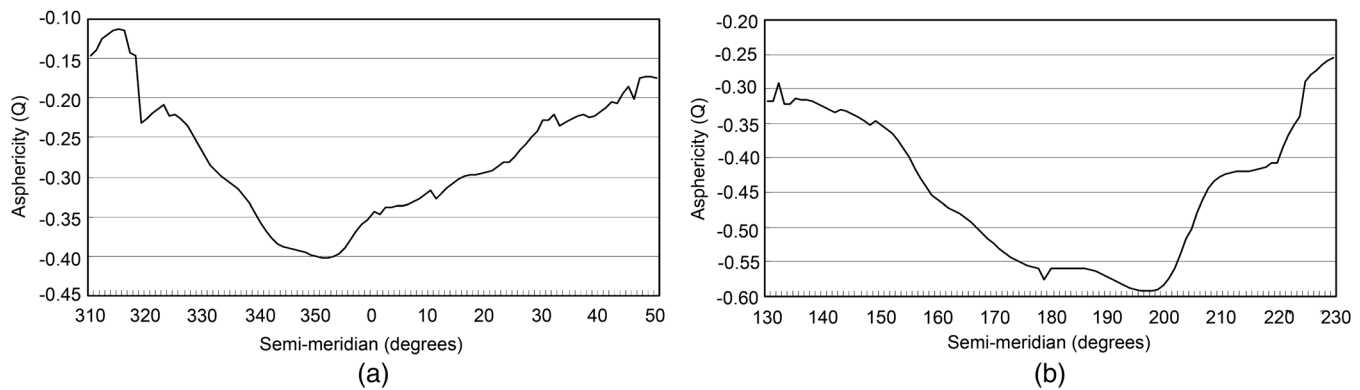
Fig. 8 Variation in asphericity as a function of semi-meridian in the nasal (a) and temporal (b) of the right cornea for subject no. 53.

the semi-meridian regions is quite moderate and smooth. It conforms to the smoothness of the corneal surface.

Figure 8 shows an example of the variation in asphericity with semi-meridian at 1-deg. intervals both in the nasal (a) and temporal (b) of the right cornea for subject no. 53. The variation trend in individual Q-value is similar to that in Fig. 6 (nasal) and Fig. 7 (temporal). The Q-values gradually become less-negative rom horizontal semi-meridians to oblique semi-meridians. The asphericity of the corneal surface gradually weakens from the horizontal to oblique meridians.

4.6 Distribution of r_0-Values by Tangential Radius

The r_0-values became smaller from horizontal semi-meridian regions to oblique semi-meridian regions in the nasal and temporal cornea. The r_0-values in the nasal cornea were much greater than those in the temporal cornea. We suggest that a corneal section with greater r_0-value has a more negative Q-value. The variation in r_0-values within semi-meridian regions is moderate and smooth.

4.7 Coefficients of Determination

The mean values of coefficients of determination (R^2) in the nasal and temporal cornea were above 0.83, which indicated that the Q-value calculation by the linear regression method was viable. In addition, the coefficient of determination for the near vertical region was poorer than the horizontal and oblique regions, which was in agreement with Douthwaite.[9] This difference may be due to problems associated with acquiring a good image or due to the upper lid inducing a non-conic form to the section. Further work is needed to study Q and r_0 for the near vertical region in order that the whole corneal shape can be presented more completely.

In summary, the method of calculating Q-values by the tangential radius of curvature could provide more reasonable and complete Q-values of anterior corneal surface than that calculated by the sagittal radius of curvature. The Q-value of any semi-meridian could be calculated by the tangential radius of curvature. This would be the basis to reconstruct the model of the whole anterior corneal surface.

References

1. K. Scholz et al., "Topography-based assessment of anterior corneal curvature and asphericity as a function of age, sex, and refractive status," *J. Cataract Refract. Surg.* **35**(6), 1046–1054 (2009).
2. M. Guillon, D. P. Lydon, and C. Wilson, "Corneal topography: a clinical model," *Ophthalmic. Physiol. Opt.* **6**(1), 47–56 (1986).
3. A. G. Bennett, "Aspherical and continuous curve contact lenses," *Optometry. Today.* **28**(1), 11–14; **28**(5), 140–142; **28**(9), 238–242; **28**(16), 433–444 (1988).
4. R. Lindsay, G. Smith, and D. Atchison, "Descriptors of corneal shape," *Optom. Vis. Sci.* **75**(2), 156–158 (1998).
5. G. Smith and D. Atchison, "Non-Gaussian optics: introduction to aberrations," Chapter 5, in *The Eye and Visual Optical Instruments*, pp. 117, Cambridge Univ. Press, New York (1997).
6. A. G. Bennett and R. B. Rabbetts, "What radius does the conventional keratometer measure?," *Ophthalmic. Physiol. Opt.* **11**(3), 239–247 (1991).
7. S. W. Cheung, P. Cho, and W. A. Douthwaite, "Corneal shape of Hong Kong-Chinese," *Ophthalmic. Physiol. Opt.* **20**(2), 119–125 (2000).
8. W. A. Douthwaite and W. T. Evardson, "Corneal topography by keratometry," *Br. J. Ophthalmol.* **84**(8), 84–847 (2000).
9. W. A. Douthwaite, "The asphericity, curvature and tilt of the human cornea measured using a videokeratoscope," *Ophthalmic. Physiol. Opt.* **23**(2), 141–150 (2003).
10. W. R. Davis et al., "Corneal asphericity and apical curvature in children: a cross-sectional and longitudinal evaluation," *Invest. Ophthalmol. Vis. Sci.* **46**(6), 1899–1906 (2005).
11. W. A. Douthwaite and E. A. Mallen, "Cornea measurement comparison with Orbscan II and EyeSys videokeratoscope," *Optom. Vis. Sci.* **84**(7), 598–604 (2007).
12. D. Gatinel, M. Haouat, and T. Hoang-Xuan, "A review of mathematical descriptors of corneal asphericity," *J. Fr. Ophtalmol.* **25**(1), 81–90 (2002).
13. C. Roberts, "Characterization of the inherent error in a spherically-biased corneal topography system in mapping a radially aspheric surface," *J. Refract Corneal. Surg.* **10**(2), 103–111 (1994).
14. C. Roberts, "Analysis of the inherent error of the TMS-1 topographic modeling system in mapping a radially aspheric surface," *Cornea.* **14**(3), 258–265 (1995).
15. J. S. Chan et al., "Accuracy of videokeratography for instantaneous radius in keratoconus," *Optom. Vis. Sci.* **72**(11), 793–799 (1995).
16. L. B. Szczotka and J. Thomas, "Comparison of axial and instantaneous videokeratographic data in keratoconus and utility in contact lens curvature prediction," *CLAO. J.* **24**(1), 22–28 (1998).
17. Bausch & Lomb, "Navigating through menu headings," Chapter 3 in *Orbscan Operator's Manual*, Version 3.0, Bausch & Lomb, Salt Lake City, UT, pp. 3–15 (2000).

18. W. A. Douthwaite, "EyeSys corneal topography measurement applied to calibrated ellipsoidal convex surfaces," *Br. J. Ophthalmol.* **79**(9), 797–801 (1995).
19. R. B. Mandell, C. S. Chiang, and S. A. Klein, "Location of the major corneal reference points," *Optom. Vis. Sci.* **72**(11), 776–784 (1995).
20. W. A. Douthwaite and A. Parkinson, "Precision of Orbscan II assessment of anterior corneal curvature and asphericity," *J. Refract. Surg.* **25**(5), 435–443 (2009).
21. British Standards Institution, *Accuracy (Trueness and Precision) of Measurement Methods and Results: Basic Methods for the Determination of Repeatability and Reproducibility of a Standard Measurement Method (BS ISO 5725-2:1994)*, British Standards Institution, London (1994).
22. L. G. Portney and M. P. Watkins, "Statistical measures of reliability," Chapter 26, in *Foundations of Clinical Research: Applications to Practice*, Prentice Hall Health, NJ (2000).
23. Y. Mejía-Barbosa and D. Malacara-Hernández, "A review of methods for measuring corneal topography," *Optom. Vis. Sci.* **78**(4), 240–253 (2001).
24. P. M. Kiely, G. Smith, and L. G. Carney, "The mean shape of the human cornea," *Optica. Acta.* **29**(8), 1027–1040 (1982).